Semileptonic decays of doubly charmed baryons in the bag model

Chao-Qiang Geng, Chia-Wei Liu, Xiao Yu, and Ao-wen Zhou

School of Fundamental Physics and Mathematical Sciences, Hangzhou Institute for Advanced Study,
UCAS, Hangzhou 310024, China
and University of Chinese Academy of Sciences, 100190 Beijing, China

We study the semileptonic decays of $B_{cc} \to B_c \ell^+ \nu_\ell$ with the bag model, where $\ell = (e, \mu)$, $B_{cc} = (\Xi_{cc}^{++}, \Xi_{cc}^+, \Omega_{cc}^+)$, and B_c are the singly charmed baryons with $J^P = 1/2^+$. We obtain the decay widths of $\Gamma(\Xi_{cc}^{++} \to \Xi_c^+ e^+ \nu_e, \Xi_c'^+ e^+ \nu_e, \Lambda_c^+ e^+ \nu_e, \Omega_c^+ e^+ \nu_e) = (5.1 \pm 0.1, 11 \pm 1, 0.34 \pm 0.06, 0.76 \pm 0.06) \times 10^{-14}$ GeV, $\Gamma(\Xi_{cc}^+ \to \Xi_c^0 e^+ \nu_e, \Xi_c'^0 e^+ \nu_e, \Sigma_c^0 e^+ \nu_e) = (5.1 \pm 0.6, 11 \pm 1, 1.5 \pm 0.1) \times 10^{-14}$ GeV, and $\Gamma(\Omega_{cc}^+ \to \Omega_c^0 e^+ \nu_e, \Xi_c^0 e^+ \nu_e, \Xi_c'^0 e^+ \nu_e) = (22 \pm 2, 0.32 \pm 0.04, 0.77 \pm 0.06) \times 10^{-14}$ GeV. We also get that $\Gamma(B_{cc} \to B_c \mu^+ \nu_\mu)/\Gamma(B_{cc} \to B_c e^+ \nu_e) = 0.97–1.00$. In addition, we discuss the $SU(3)$ flavor breaking effects, classified into three aspects: phase space differences, spectator quarks, and overlappings of the transited quarks. In particular, we show that the breaking effects are dominated by the phase space differences, which can be as large as 25%. Explicitly, we find that $\Gamma(\Xi_{cc}^{++} \to \Lambda_c^+ e^+ \nu_e) V_{cs}^2 / \Gamma(\Xi_{cc}^{++} \to \Xi_c^+ e^+ \nu_e) V_{cd}^2 = 1.24$, which is expected as 1 under the exact $SU(3)$ flavor symmetry.

I. INTRODUCTION

In 2002, the SELEX Collaboration reported a resonant structure in $\Lambda_c^+ K^- \pi^+$ and pD^+K^- [1,2], which can be potentially caused by $\Xi_{cc}^+(3620)$. However, the same structure was not confirmed by the FOCUS, *BABAR*, and BELLE Collaborations [3–5]. Eventually, the long-awaited evidence finally arrived in 2017 via $\Xi_{cc}^{++} \to \Lambda_c^+ K^- \pi^+ \pi^+$ at LHCb [6], where the mass is determined to be

$$M_{\Xi_{cc}^{++}} = (3621.40 \pm 0.72 \pm 0.27 \pm 0.14) \text{ MeV.} \quad (1)$$

This encouraging finding was soon accompanied by the lifetime measurement of Ξ_{cc}^{++} [7] as well as the observation of $\Xi_{cc}^{++} \to \Xi_c^+ \pi^+$ [8]. One can reasonably expect much more experimental results in the future, providing opportunities to deepen our knowledge of hadron physics.

On the theoretical aspect, the low-lying charmed baryons are categorized by the representations of the flavor $SU(3)$ $(SU(3)_F)$ symmetry, given in Fig. 1. Under $SU(3)_F$, the doubly charmed baryons (B_{cc}) form a triplet, while the singly charmed baryons (B_c) consist of a antitriplet and a sextet. Their masses and magnetic dipole moments are intensively studied within the quark models [9–21]. In addition, to deal with the weak decays, lots of approaches have also been

performed [22–42]. In the diquark approach, two of the three quarks are grouped as a diquark cluster, simplifying the problem to a two-body one [12,13,35–37,43]. Nonetheless, it is unclear which quarks shall form a diquark cluster. On the other hand, the problem does not exist in the MIT bag model (MBM), as a diquark cluster is unnecessary.

The MBM describes hadrons at rest as localized objects. Along with the bag and zero point energies, the model is suitable to explain the mass spectra. However, it becomes problematic in the decays due to the unwanted center-of-mass motion. This problem can be understood by the Heisenberg uncertainty principle, which states that a localized object can not possess a definite momentum. If we treat a bag state as a baryon at rest, the calculations will not respect the energy-momentum conservation. The problem was tackled a few years ago by taking the linear superposition of infinite bags in Ref. [44]. This approach has been applied to various decay systems [45–49].

This paper is organized as follows. We present the formalism of the decay branching fractions in terms of the helicity amplitudes in Sec. II. In Sec. III, we give our numerical results and compare them with those in the literature. We summarize this work in Sec. IV.

II. FORMALISM

The effective Hamiltonian for the transitions of $c \to f \ell^+ \nu$ ($f = d, s$) at the quark level is given as

$$\mathcal{H}_{\text{eff}} = \frac{G_F}{\sqrt{2}} V_{cf} \bar{\ell} \gamma^\mu (1 - \gamma_5) \nu_\ell \bar{f} \gamma_\mu (1 - \gamma_5) c, \quad (2)$$
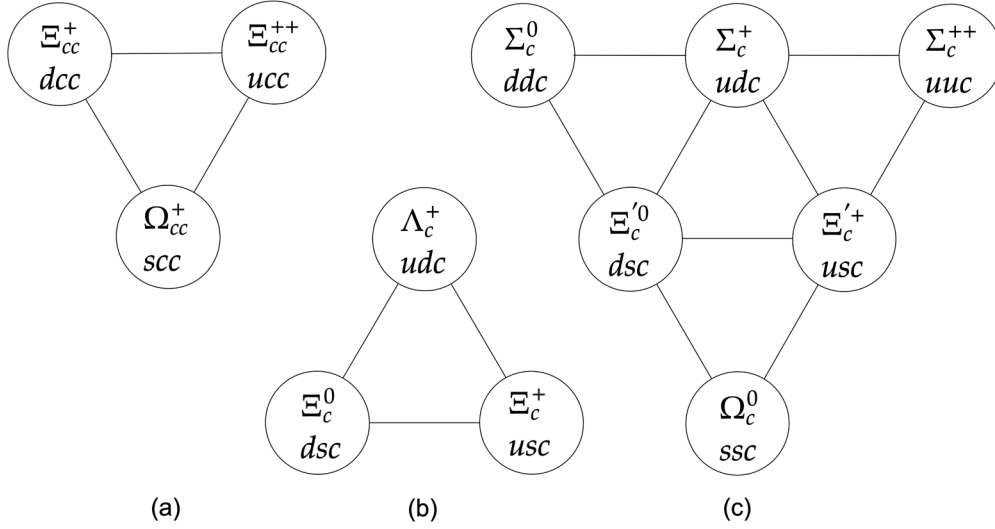
FIG. 1. Quark states of the charmed baryons, where (a) represents an $SU(3)_F$ triplet with the doubly charmed baryons, while (b) and (c) correspond to the $SU(3)_F$ antitriplet and sextet with the singly charmed baryons, respectively.

where G_F is the Fermi constant, and V_{cf} corresponds to the Cabibbo-Kobayashi-Maskawa matrix elements. The weak transition amplitudes of the doubly charmed baryons are then given as

$$\mathcal{A}(B_{cc} \to B_c \ell^+ \nu_\ell) = \frac{G_F}{\sqrt{2}} V_{cq} \bar{\ell} \gamma^\mu (1 - \gamma_5) \nu_\ell \langle B_c, p_f | \bar{f} \gamma_\mu (1 - \gamma_5) c | B_{cc}, p_i \rangle, \tag{3}$$

with the baryon matrix elements parametrized by

$$\langle B_c, p_f, \lambda_f | \bar{f} \gamma_\mu (1 - \gamma_5) c | B_{cc}, p_i, \lambda_i \rangle = \bar{u}_f(p_f, \lambda_f) \left[\gamma_\mu f_1(q^2) - i\sigma_{\mu\nu} \frac{q^\nu}{M_i} f_2(q^2) + f_3(q^2) \frac{q_\mu}{M_i} \right] u_i(p_i, \lambda_i)$$

$$- \bar{u}_f(p_f, \lambda_f) \left[\gamma_\mu g_1(q^2) - i\sigma_{\mu\nu} \frac{q^\nu}{M_i} g_2(q^2) + g_3(q^2) \frac{q_\mu}{M_i} \right] \gamma_5 u_i(p_i, \lambda_i), \tag{4}$$

where $f_{123}(q^2)$ and $g_{123}(q^2)$ are the form factors, $\sigma^{\mu\nu} = i[\gamma^\mu, \gamma^\nu]/2$, $q_\mu = p_i^\mu - p_f^\mu$, and $\lambda_{f(i)}$, $p_{f(i)}^\mu$, $M_{f(i)}$ and $u_{f(i)}$ are the helicity, four-momentum, mass and Dirac spinor of $B_{c(c)}$, respectively.

In order to calculate the decay widths, we introduce a set of helicity amplitudes $H_{\lambda_f \lambda_W}^{V(A)}$, where λ_f and λ_W represent the helicity quantum numbers of B_c and the off-shell W^+ boson, respectively. Relations between the helicity amplitudes and form factors are given by [50]

$$H_{\frac{1}{2}1}^V = \sqrt{2Q_-} \left(-f_1(q^2) - \frac{M_i + M_f}{M_i} f_2(q^2) \right),$$

$$H_{\frac{1}{2}0}^V = \frac{\sqrt{Q_-}}{q^2} \left((M_i + M_f) f_1(q^2) + \frac{q^2}{M_i} f_2(q^2) \right),$$

$$H_{\frac{1}{2}t}^V = \frac{\sqrt{Q_+}}{q^2} \left((M_i - M_f) f_1(q^2) + \frac{q^2}{M_i} f_3(q^2) \right),$$

$$H_{\frac{1}{2}1}^A = \sqrt{2Q_+} \left(g_1(q^2) - \frac{M_i - M_f}{M_i} g_2(q^2) \right),$$

$$H_{\frac{1}{2}0}^A = \frac{\sqrt{Q_+}}{q^2} \left(-(M_i - M_f) g_1(q^2) + \frac{q^2}{M_i} g_2(q^2) \right),$$

$$H_{\frac{1}{2}t}^A = \frac{\sqrt{Q_-}}{q^2} \left(-(M_i + M_f) g_1(q^2) + \frac{q^2}{M_i} g_3(q^2) \right), \tag{5}$$

where $Q_\pm = (M_i \pm M_f)^2 - q^2$ and $H^{V(A)}_{\lambda_f \lambda_W} = (-)H^{V(A)}_{-\lambda_f -\lambda_W}$. The differential decay widths are given in terms of the helicity amplitudes as [50–52]

$$\partial_q \Gamma = \frac{\partial \Gamma}{\partial q^2} = \frac{1}{3} \frac{G_F^2}{(2\pi)^3} |V_{fc}|^2 \frac{(q^2 - m_\ell^2)^2 p}{8M_i^2 q^2} \left[\left(1 + \frac{m_\ell^2}{2q^2}\right) \left(|H_{\frac{1}{2}1}|^2 + |H_{-\frac{1}{2}-1}|^2 + |H_{\frac{1}{2}0}|^2 + |H_{-\frac{1}{2}0}|^2 \right) + \frac{3m_\ell^2}{2q^2} \left(|H_{\frac{1}{2}t}|^2 + |H_{-\frac{1}{2}t}|^2 \right) \right], \tag{6}$$

where $p = \sqrt{Q^+ Q^-}/2M_{B_i}$, $H_{\lambda_f \lambda_W} = H^V_{\lambda_f \lambda_W} - H^A_{\lambda_f \lambda_W}$ and m_ℓ is the lepton mass.

In this work, we evaluate the form factors with the homogeneous bag model (HBM) [49]. The baryon wave functions of B_{cc} are given as

$$|B_{cc}, \updownarrow\rangle = \int \frac{1}{2\sqrt{3}} \epsilon^{\alpha\beta\gamma} q'^\dagger_{a\alpha}(\vec{x}_1) c^\dagger_{b\beta}(\vec{x}_2) c^\dagger_{c\gamma}(\vec{x}_3) \Psi^{abc}_{A_\updownarrow(ucc)}(\vec{x}_1, \vec{x}_2, \vec{x}_3) [d^3\vec{x}] |0\rangle, \tag{7}$$

where $q' = (u, d, s)$ for $B_{cc} = (\Xi^{++}_{cc}, \Xi^+_{cc}, \Omega^+_{cc})$, $q'^\dagger$ and $c^\dagger$ represent the creation operators of quarks, the Latin and Greek letters stand for the Dirac spinor and color indices, and Ψ_A are the spatial wave functions defined in Refs. [47–49], respectively. On the other hand, the wave functions of B_c can be found in Ref. [47].

We choose the Breit frame to calculate the baryon matrix elements, where B_c and B_{cc} have the opposite velocities $\vec{v} = v\hat{z}$ and $-\vec{v}$. The baryon matrix elements of the current operators are then governed by

$$\langle B_c(\vec{v}), \lambda_f | f^\dagger \Upsilon c(0) | B_{cc}(-\vec{v}), \lambda_i \rangle = \mathcal{N}_{B_c} \mathcal{N}_{B_{cc}} \int d^3\vec{x}_\triangle \Upsilon^{\lambda_f \lambda_i}_{fc}(\vec{x}_\triangle) \prod_{q=c,q'} D^v_q(\vec{x}_\triangle),$$

$$D^v_q(\vec{x}_\triangle) = \frac{1}{\gamma} \int d^3\vec{x} \phi^\dagger_q\left(\vec{x} + \frac{1}{2}\vec{x}_\triangle\right) \phi_q\left(\vec{x} - \frac{1}{2}\vec{x}_\triangle\right) e^{-2iE_q vz},$$

$$\Upsilon^{\lambda_f \lambda_i}_{fc}(\vec{x}_\triangle) = \sum_{\lambda_q \lambda_c} N^{\lambda_f \lambda_i}_{\lambda_q \lambda_c} \int d^3\vec{x} \phi^\dagger_{f\lambda_q}(\vec{x}^+) S_{\vec{v}} \Upsilon S_{-\vec{v}} \phi_{c\lambda_c}(\vec{x}^-) e^{2i(E_{q'}+E_c)\vec{v}\cdot\vec{x}}, \tag{8}$$

where $\mathcal{N}_{B_c, B_{cc}}$ are the normalization constants, Υ is an arbitrary Dirac matrix, $\vec{x}^\pm = \vec{x} \pm \vec{x}_\triangle/2$, ϕ_q are the bag wave functions in the MBM, $S_{\pm v} = a_+ \pm a_- \gamma^0 \gamma^3$ with $a_\pm = \sqrt{1 \pm \gamma^2}$ and $\gamma = 1/\sqrt{1 - v^2}$, and $\lambda_{q,c} \in \{\uparrow, \downarrow\}$. The derivations of Eq. (8) and the explicit forms of ϕ_q are given in Ref. [49]. The first line of Eq. (8) is the total overlapping between B_{cc} and B_c induced by $f^\dagger \Upsilon c(0)$ at the quark level, while the second and third terms are interpreted as

  (i) The spectator quark effects are governed by $D^v_q(\vec{x}_\triangle)$, which describe the overlapping of q in two bag states separated by $\vec{x}_\triangle$.

  (ii) The quark transitions are described by $\Upsilon^{\lambda_f \lambda_i}_{fc}$, where $N^{\lambda_f, \lambda_i}_{\lambda_q, \lambda_c}$ are the spin-flavor overlapping coefficients.

In the heavy constituent quark limit ($m_{u,d,c} \to \infty$), the formalism is reduced to

$$\langle B_c(\vec{v}), \uparrow | f^\dagger c(0) | B_{cc}(-\vec{v}), \uparrow \rangle = \sum_{\lambda_q \lambda_c} N^{\uparrow\uparrow}_{\lambda_q \lambda_c},$$

$$\langle B_c(\vec{v}), \uparrow | f^\dagger \gamma^0 \gamma^1 \gamma_5 c(0) | B_{cc}(-\vec{v}), \downarrow \rangle = \sum_{\lambda_q \lambda_c} N^{\uparrow\downarrow}_{\lambda_q \lambda_c}. \tag{9}$$

From the angular momentum conservation, we have that

$$N^{\lambda_f \lambda_i}_{\lambda_q \lambda_c} = 0 \quad \text{for } \lambda_f - \lambda_i \neq \lambda_c - \lambda_q. \tag{10}$$

It states that if the baryon spin is (un)flipped by the operator, then the spin of the quark shall also be (un)flipped. In addition, by the Wiger-Eckart theorem, we find that

$$N^{\uparrow\uparrow}_{\lambda_q \lambda_c} = N^{\downarrow\downarrow}_{-\lambda_q -\lambda_c}, \qquad N^{\uparrow\uparrow}_{\uparrow\uparrow} - N^{\uparrow\uparrow}_{\downarrow\downarrow} = N^{\downarrow\downarrow}_{\downarrow\downarrow} = N^{\uparrow\downarrow}_{\uparrow\downarrow}. \tag{11}$$

Consequently, there are only two independent numbers given as

$$N_{\text{unflip}} \equiv N^{\uparrow\uparrow}_{\uparrow\uparrow} + N^{\uparrow\uparrow}_{\downarrow\downarrow}, \qquad N_{\text{flip}} \equiv N^{\uparrow\downarrow}_{\downarrow\uparrow}, \tag{12}$$

which are collected in Table I.

TABLE I. The spin-flavor overlappings of $B_{cc} \to B_c$.

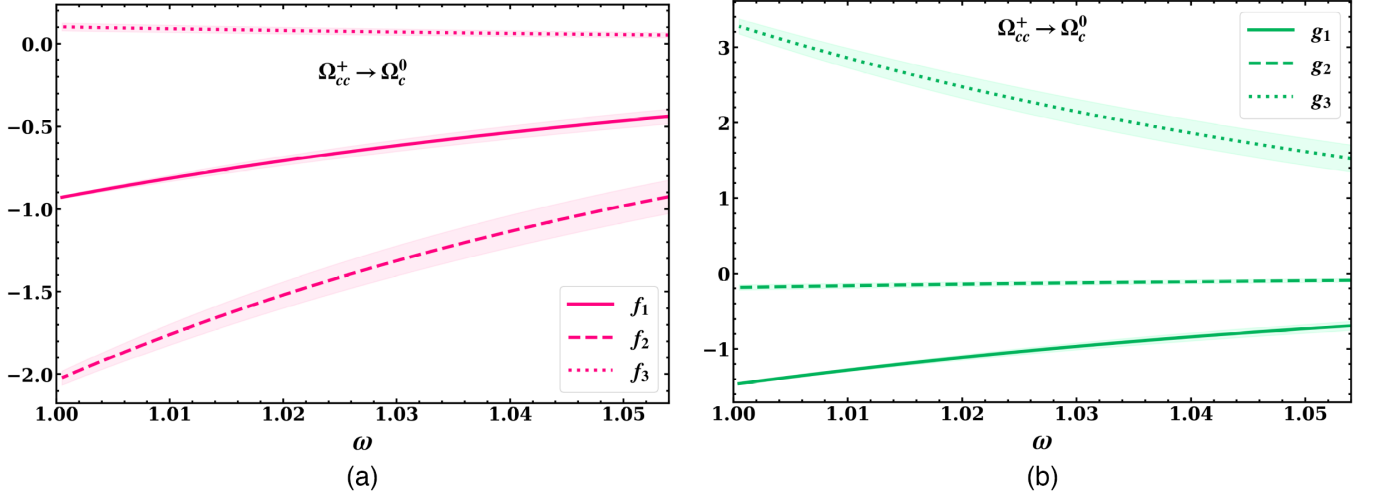| $c \to s$	N_{unflip}	N_{flip}	$c \to d$	N_{unflip}	N_{flip}
$\Xi^{++}_{cc} \to \Xi^+_c$	$\frac{\sqrt{6}}{2}$	$\frac{\sqrt{6}}{6}$	$\Xi^{++}_{cc} \to \Lambda^+_c$	$\frac{\sqrt{6}}{2}$	$\frac{\sqrt{6}}{6}$
$\Xi^+_{cc} \to \Xi^0_c$	$\frac{\sqrt{6}}{2}$	$\frac{\sqrt{6}}{6}$	$\Omega^+_{cc} \to \Xi^0_c$	$\frac{\sqrt{6}}{2}$	$\frac{\sqrt{6}}{6}$
$\Xi^{++}_{cc} \to \Xi'^+_c$	$-\frac{\sqrt{2}}{2}$	$-\frac{5\sqrt{2}}{6}$	$\Xi^{++}_{cc} \to \Sigma^+_c$	$-\frac{\sqrt{2}}{2}$	$-\frac{5\sqrt{2}}{6}$
$\Xi^+_{cc} \to \Xi'^0_c$	$-\frac{\sqrt{2}}{2}$	$-\frac{5\sqrt{2}}{6}$	$\Omega^+_{cc} \to \Xi'^0_c$	$-\frac{\sqrt{2}}{2}$	$-\frac{5\sqrt{2}}{6}$
$\Omega^+_{cc} \to \Omega^0_c$	-1	$-\frac{5}{3}$	$\Xi^+_{cc} \to \Sigma^0_c$	-1	$-\frac{5}{3}$

FIG. 2. The form factors of $\Omega_{cc}^+ \to \Omega_c$ as functions of ω, where the center lines and bands correspond to the central values and uncertainties, respectively.

III. NUMERICAL RESULTS

The values of V_{cf} are given by [53]

$$|V_{cs}| = 0.987 \pm 0.011, \qquad |V_{cd}| = 0.221 \pm 0.004, \quad (13)$$

while the model parameters are taken as [49]

$$R = 4.7 \pm 0.3 \text{ GeV}^{-1}, \qquad m_c = 1.655 \text{ GeV},$$
$$m_{u,d} = 0, \qquad m_s = 0.2 \pm 0.1 \text{ GeV}. \quad (14)$$

Notice that B_{cc} and B_c have different bag radii, found to be around 4.4 and 5.0 GeV^{-1}, respectively [54]. However, to simplify the formalism, we take their bag radii as equal and allow them to vary from 4.4 to 5.0 GeV^{-1}.

To illustrate the recoil effects of the form factors, we plot those of $\Omega_{cc}^+ \to \Omega_c$ in Fig. 2. We define

$$\omega \equiv \frac{M_i^2 + M_f^2 - q^2}{2M_i M_f} = \frac{1 + v^2}{1 - v^2}, \quad (15)$$

so that the zero recoil point $(q^2 = q_{\max}^2 = (M_i - M_f)^2)$ corresponds to $\omega = 1$ for all the decays. As shown in the figures, f_3 and g_2 can be taken as zero practically. The uncertainties of f_1 and g_1 are negligible at the low q^2 regions, and around 10% at $\omega = 1.06$. As a result, at $\omega = 1$, f_1 and g_1 are not polluted by the uncertainties of the quark energies. However, the uncertainties of f_2 and g_3 are large in all regions.

The form factors of $\Xi_{cc}^{++} \to B_c$ at $q^2 = 0$, along with those in the literature, are given in Table II. For completeness, we also show all our calculated values of the form factors for $\Xi_{cc}^{++} \to B_c$ with the HBM in Table III. Note that the form factors of $\Xi_{cc}^{++} \to \Xi_c^+$ and $\Xi_{cc}^+ \to \Xi_c^0$ are

the same due to the isospin symmetry. Compared to those in the literature, our form factors of $\Xi_{cc}^{++} \to \Lambda_c^+$ have an overall minus sign due to the convention on the baryon wave functions, which does not affect the physical quantities. Note that our results of the form factors at $q^2 = 0$ are significantly smaller than those in other approaches.

In Figs. 3(a) and 3(b), we compare the form factors of $\Xi_{cc}^{++} \to \Xi_c^+$ and $\Xi_{cc}^{++} \to \Lambda_c^+$, corresponding to $c \to s$ and $c \to d$ transitions, respectively. These form factors shall be identical in the limit of the $SU(3)_F$ symmetry. The figures show that for a fixed value of ω, the form factors are

TABLE II. The form factors of Ξ_{cc}^{++} calculated in the HBM, light-front quark model (LFQM), and QCD sum rule (QCDSR) at $q^2 = 0$.

	HBM (This work)	LFQM [26,42]	QCDSR [39,40,42]
$f_1^{\Xi_{cc}^{++} \to \Lambda_c^+}$	0.28 ± 0.05	-0.79	-0.59 ± 0.05
$f_2^{\Xi_{cc}^{++} \to \Lambda_c^+}$	-0.01 ± 0.01	0.008	0.039 ± 0.024
$f_3^{\Xi_{cc}^{++} \to \Lambda_c^+}$	-0.16 ± 0.02	$\cdots$	0.35 ± 0.11
$g_1^{\Xi_{cc}^{++} \to \Lambda_c^+}$	0.09 ± 0.02	-0.22	-0.13 ± 0.08
$g_2^{\Xi_{cc}^{++} \to \Lambda_c^+}$	0.01 ± 0.00	0.05	0.037 ± 0.027
$g_3^{\Xi_{cc}^{++} \to \Lambda_c^+}$	-0.21 ± 0.02	$\cdots$	0.31 ± 0.09
$f_1^{\Xi_{cc}^{++} \to \Sigma_c^+}$	-0.24 ± 0.01	-0.47	-0.35 ± 0.04
$f_2^{\Xi_{cc}^{++} \to \Sigma_c^+}$	-0.53 ± 0.05	1.04	1.15 ± 0.12
$f_3^{\Xi_{cc}^{++} \to \Sigma_c^+}$	0.03 ± 0.00	$\cdots$	-1.40 ± 0.39
$g_1^{\Xi_{cc}^{++} \to \Sigma_c^+}$	-0.37 ± 0.05	-0.62	-0.23 ± 0.06
$g_2^{\Xi_{cc}^{++} \to \Sigma_c^+}$	-0.05 ± 0.00	0.05	-0.26 ± 0.15
$g_3^{\Xi_{cc}^{++} \to \Sigma_c^+}$	0.89 ± 0.06	$\cdots$	2.68 ± 0.39

approximately the same. Explicitly, their values deviate by less than 13%. However, the phase space of the $c \to s$ transition is about 30% smaller than the one of $c \to d$. As shown in the figures, the form factors of $\Xi_{cc}^{++} \to \Xi_c^+$ with $\omega > 1.07$ are missing as they correspond to the region of $q^2 < 0$.

On the other hand, to examine the spectator effects, we plot the results of $\Xi_{cc}^{++} \to \Sigma_c^+$ and $\Omega_{cc}^+ \to \Xi_c^0$ in Figs. 3(c) and 3(d), corresponding to the $c \to d$ transition with (c, u) and (c, s) as the spectator quarks, respectively. We find that the form factors deviate less than 11% between the two types of transition. We conclude that the form factors well respect the $SU(3)_F$ symmetry if one uses the variables of ω instead of q^2.

The total decay widths of Γ are computed by integrating Eq. (6). To further examine the results, we decompose the decay widths into four fragments, given by

$$P_1 = \frac{1}{\Gamma} \int_{m_e^2}^{\frac{1}{4}q_{max}^2} \partial_q \Gamma dq^2, \qquad P_2 = \frac{1}{\Gamma} \int_{\frac{1}{4}q_{max}^2}^{\frac{1}{2}q_{max}^2} \partial_q \Gamma dq^2,$$

$$P_3 = \frac{1}{\Gamma} \int_{\frac{1}{2}q_{max}^2}^{\frac{3}{4}q_{max}^2} \partial_q \Gamma dq^2, \qquad P_4 = \frac{1}{\Gamma} \int_{\frac{3}{4}q_{max}^2}^{q_{max}^2} \partial_q \Gamma dq^2, \quad (16)$$

with their values listed in Table IV, respectively. The uncertainties of P_i are tiny compared to the total branching fractions due to the correlations. In addition, we find that except for $\Xi_{cc}^{++} \to \Xi_c^+ e^+ \nu_e$, the values of P_1 are the smallest among the fragments. In contrast to the others, the decay width of $\Xi_{cc}^{++} \to \Xi_c^+ e^+ \nu_e$ distributes smoothly among the four regions.

In Fig. 4, we plot the differential decay widths. In the high q^2 areas, the uncertainties are minor since f_1 and g_1 have few errors, as explained at the beginning of this section. We see that $\partial_q \Gamma(\Xi_{cc}^{++} \to \Xi_c^+ e^+ \nu_e)$ is much

TABLE III. The form factors from the HBM with $\Xi_c^{(\prime)} = (\Xi_c^{(\prime)+}, \Xi_c^{(\prime)0})$ for $\Xi_{cc} = (\Xi_{cc}^{++}, \Xi_{cc}^+)$.

	$q^2 = 0$	$q^2 = q_{max}^2$		$q^2 = 0$	$q^2 = q_{max}^2$
$f_1^{\Xi_{cc} \to \Xi_c}$	0.45 ± 0.05	1.36 ± 0.00	$g_1^{\Xi_{cc} \to \Xi_c}$	0.14 ± 0.02	0.38 ± 0.00
$f_2^{\Xi_{cc} \to \Xi_c}$	-0.03 ± 0.00	-0.15 ± 0.01	$g_2^{\Xi_{cc} \to \Xi_c}$	0.01 ± 0.00	0.03 ± 0.01
$f_3^{\Xi_{cc} \to \Xi_c}$	-0.20 ± 0.04	-0.56 ± 0.03	$g_3^{\Xi_{cc} \to \Xi_c}$	-0.28 ± 0.04	-0.79 ± 0.02
$f_1^{\Xi_{cc} \to \Xi_c'}$	-0.31 ± 0.03	-0.70 ± 0.00	$g_1^{\Xi_{cc} \to \Xi_c'}$	-0.49 ± 0.04	-1.10 ± 0.01
$f_2^{\Xi_{cc} \to \Xi_c'^+}$	-0.63 ± 0.07	-1.48 ± 0.02	$g_2^{\Xi_{cc} \to \Xi_c'}$	-0.06 ± 0.02	-0.13 ± 0.02
$f_3^{\Xi_{cc} \to \Xi_c'^+}$	0.03 ± 0.01	0.06 ± 0.02	$g_3^{\Xi_{cc} \to \Xi_c'}$	1.00 ± 0.12	2.31 ± 0.05
$f_1^{\Omega_{cc}^+ \to \Omega_c^0}$	-0.48 ± 0.04	-0.99 ± 0.00	$g_1^{\Omega_{cc}^+ \to \Omega_c^0}$	-0.69 ± 0.06	-1.56 ± 0.02
$f_2^{\Omega_{cc}^+ \to \Omega_c^0}$	-0.93 ± 0.10	-2.17 ± 0.03	$g_2^{\Omega_{cc}^+ \to \Omega_c^0}$	-0.09 ± 0.02	-0.20 ± 0.04
$f_3^{\Omega_{cc}^+ \to \Omega_c^0}$	0.05 ± 0.02	0.11 ± 0.02	$g_3^{\Omega_{cc}^+ \to \Omega_c^0}$	1.52 ± 0.18	3.51 ± 0.08
$f_1^{\Xi_{cc}^{++} \to \Lambda_c^+}$	0.28 ± 0.05	1.42 ± 0.02	$g_1^{\Xi_{cc}^{++} \to \Lambda_c^+}$	0.09 ± 0.02	0.37 ± 0.00
$f_2^{\Xi_{cc}^{++} \to \Lambda_c^+}$	-0.01 ± 0.01	-0.16 ± 0.01	$g_2^{\Xi_{cc}^{++} \to \Lambda_c^+}$	0.01 ± 0.00	0.02 ± 0.01
$f_3^{\Xi_{cc}^{++} \to \Lambda_c^+}$	-0.16 ± 0.02	-0.73 ± 0.06	$g_3^{\Xi_{cc}^{++} \to \Lambda_c^+}$	-0.21 ± 0.02	-0.91 ± 0.05
$f_1^{\Omega_{cc}^+ \to \Xi_c^0}$	0.33 ± 0.05	1.41 ± 0.02	$g_1^{\Omega_{cc}^+ \to \Xi_c^0}$	0.10 ± 0.02	0.37 ± 0.00
$f_2^{\Omega_{cc}^+ \to \Xi_c^0}$	-0.01 ± 0.01	-0.11 ± 0.02	$g_2^{\Omega_{cc}^+ \to \Xi_c^0}$	0.01 ± 0.00	0.04 ± 0.01
$f_3^{\Omega_{cc}^+ \to \Xi_c^0}$	-0.20 ± 0.02	-0.75 ± 0.06	$g_3^{\Omega_{cc}^+ \to \Xi_c^0}$	-0.26 ± 0.03	-0.99 ± 0.06
$f_1^{\Xi_{cc}^{++} \to \Sigma_c^+}$	-0.24 ± 0.01	-0.70 ± 0.00	$g_1^{\Xi_{cc}^{++} \to \Sigma_c^+}$	-0.37 ± 0.05	-1.08 ± 0.01
$f_2^{\Xi_{cc}^{++} \to \Sigma_c^+}$	-0.53 ± 0.05	-1.65 ± 0.7	$g_2^{\Xi_{cc}^{++} \to \Sigma_c^+}$	-0.05 ± 0.00	-0.16 ± 0.03
$f_3^{\Xi_{cc}^{++} \to \Sigma_c^+}$	0.03 ± 0.00	0.09 ± 0.02	$g_3^{\Xi_{cc}^{++} \to \Sigma_c^+}$	0.89 ± 0.06	2.71 ± 0.16
$f_1^{\Omega_{cc}^+ \to \Xi_c'^0}$	-0.24 ± 0.03	-0.70 ± 0.01	$g_1^{\Omega_{cc}^+ \to \Xi_c'^0}$	-0.37 ± 0.05	-1.08 ± 0.01
$f_2^{\Omega_{cc}^+ \to \Xi_c'^0}$	-0.56 ± 0.05	-1.71 ± 0.07	$g_2^{\Omega_{cc}^+ \to \Xi_c'^0}$	-0.06 ± 0.00	-0.17 ± 0.03
$f_3^{\Omega_{cc}^+ \to \Xi_c'^0}$	0.04 ± 0.00	0.11 ± 0.02	$g_3^{\Omega_{cc}^+ \to \Xi_c'^0}$	0.97 ± 0.07	2.92 ± 0.18
$f_1^{\Xi_{cc}^+ \to \Sigma_c^0}$	-0.38 ± 0.05	-0.95 ± 0.03	$g_1^{\Xi_{cc}^+ \to \Sigma_c^0}$	-0.52 ± 0.07	-1.47 ± 0.05
$f_2^{\Xi_{cc}^+ \to \Sigma_c^0}$	-0.75 ± 0.07	-2.23 ± 0.00	$g_2^{\Xi_{cc}^+ \to \Sigma_c^0}$	-0.07 ± 0.00	-0.21 ± 0.03
$f_3^{\Xi_{cc}^+ \to \Sigma_c^0}$	0.05 ± 0.01	0.12 ± 0.03	$g_3^{\Xi_{cc}^+ \to \Sigma_c^0}$	1.26 ± 0.09	3.67 ± 0.07
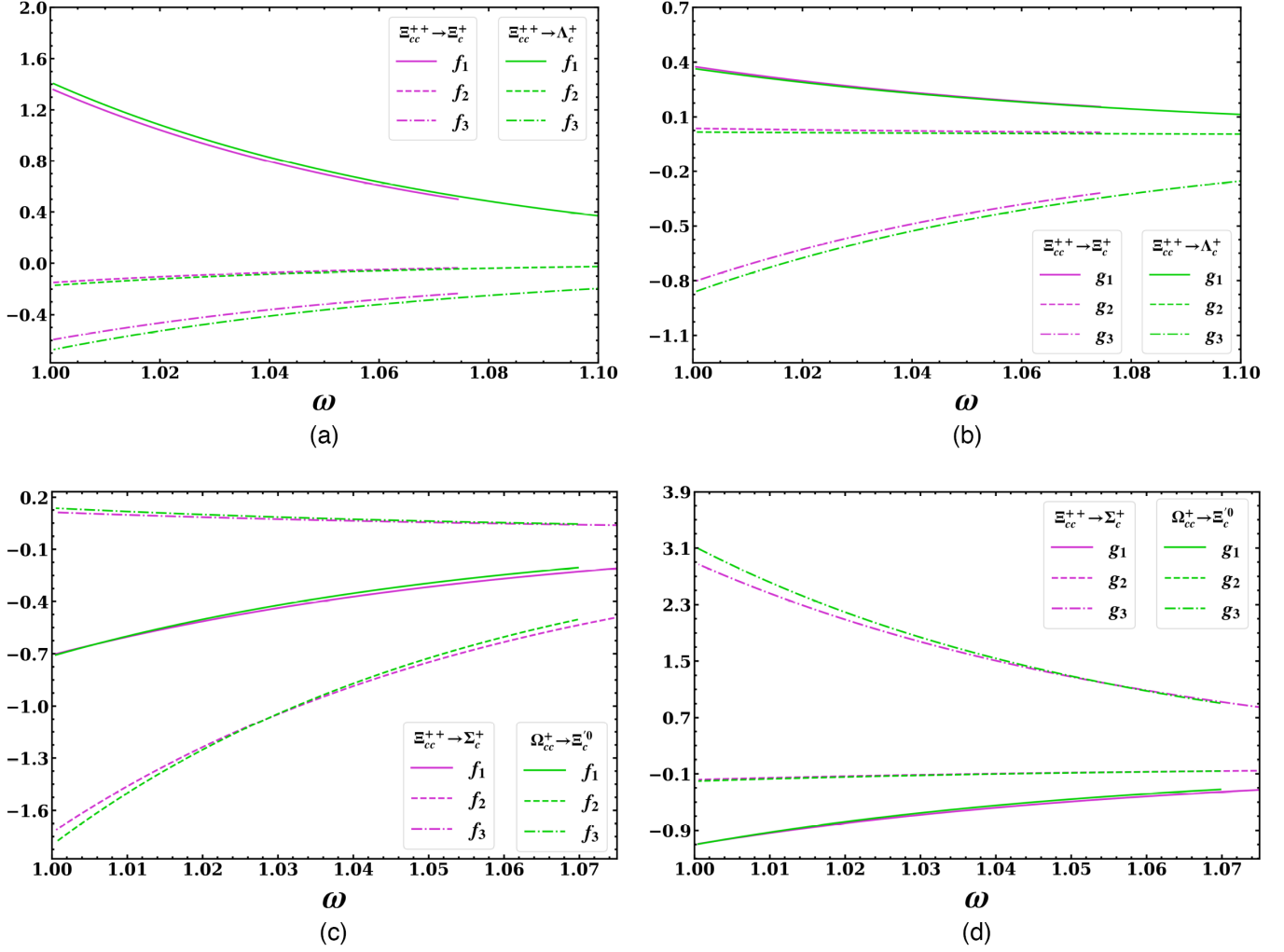
FIG. 3.   The ω dependencies of the $B_{cc} \to B_c$ form factors.

smoother than the others. To see the underlying reason, we define the parity conserving and violating partial decay widths as

$$P_C \equiv \partial_q \Gamma(g_i = 0), \quad P_V \equiv \partial_q \Gamma(f_i = 0), \quad \partial_q \Gamma = P_C + P_V,$$

$$(17)$$

where in $P_{C(V)}$ we take $g_{1,2,3}(f_{1,2,3})$ as zero, corresponding to the parity conserving (violating) parts of the decay widths. We show $P_{C,V}(\Xi_{cc}^{++} \to \Xi_c^{(\prime)+})$ in Fig. 5.

We see that $P_{C,V}$ have very different behaviors. On the one hand, P_C contribute to Γ mostly in the low q^2 regions, and their values decrease quickly as q^2 goes up. On the other hand, P_V behave oppositely. In $\Xi_{cc}^+ \to \Xi_c^+ e^+ \nu_e$, the

TABLE IV.   The total and fragmentary decay widths.

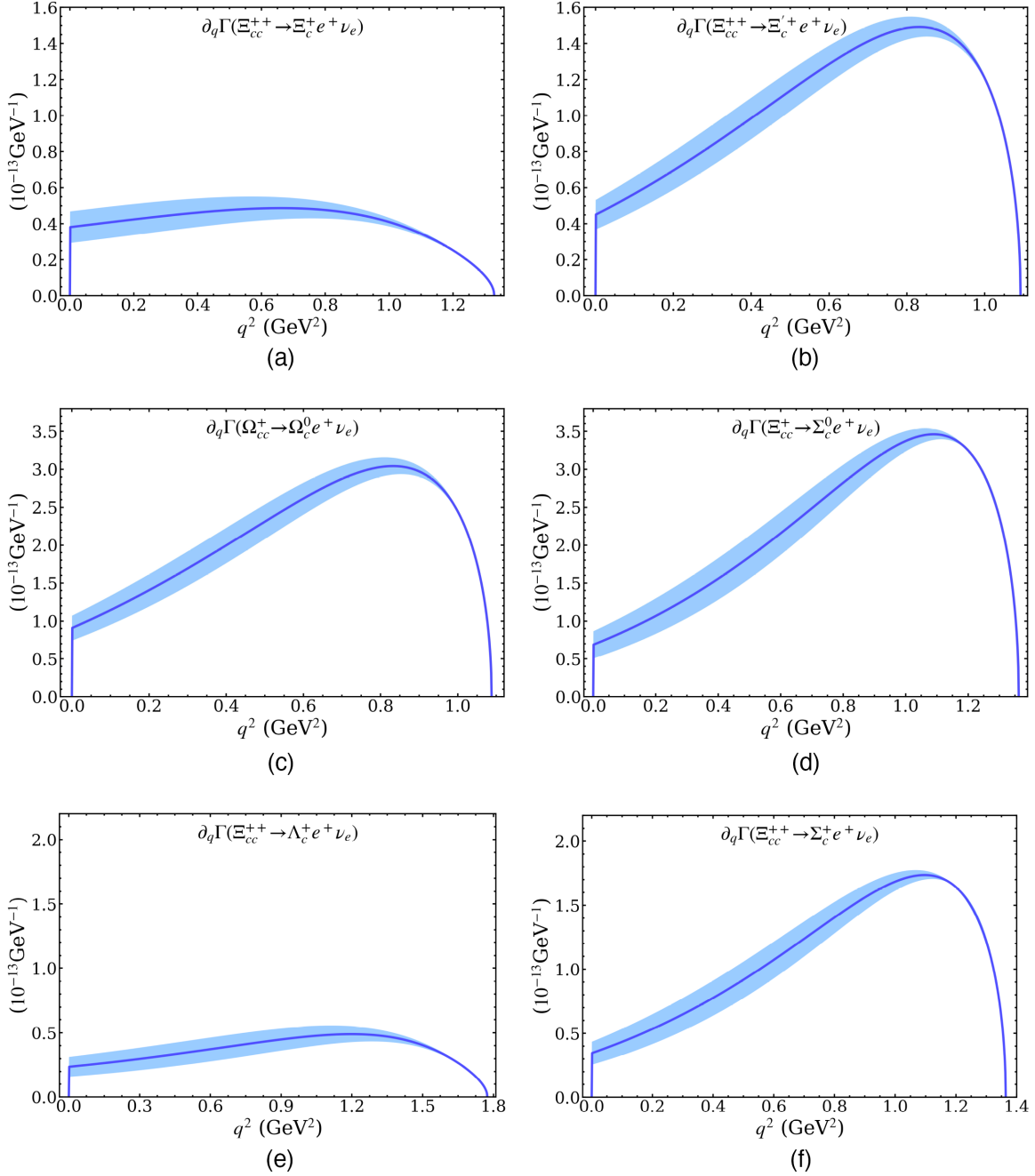| Channels	$\Gamma \times 10^{14}$ GeV^{-1}	P_1	P_2	P_3	P_4
$\Xi_{cc}^{++} \to \Xi_c^+ e^+ \nu_e$	5.11 ± 0.64	0.25 ± 0.02	0.29 ± 0.01	0.29 ± 0.01	0.17 ± 0.02
$\Xi_{cc}^{++} \to \Xi_c^{\prime+} e^+ \nu_e$	10.9 ± 0.8	0.14 ± 0.01	0.24 ± 0.01	0.33 ± 0.00	0.29 ± 0.02
$\Omega_{cc}^+ \to \Omega_c^0 e^+ \nu_e$	22.1 ± 1.6	0.14 ± 0.01	0.24 ± 0.01	0.33 ± 0.00	0.29 ± 0.02
$\Xi_{cc}^{++} \to \Lambda_c^+ e^+ \nu_e$	0.34 ± 0.06	0.17 ± 0.03	0.26 ± 0.01	0.32 ± 0.00	0.24 ± 0.04
$\Xi_{cc}^{++} \to \Sigma_c^+ e^+ \nu_e$	0.76 ± 0.06	0.12 ± 0.02	0.21 ± 0.01	0.34 ± 0.00	0.34 ± 0.03
$\Xi_{cc}^+ \to \Sigma_c^0 e^+ \nu_e$	1.52 ± 0.12	0.12 ± 0.02	0.21 ± 0.02	0.34 ± 0.00	0.34 ± 0.03

FIG. 4. The partial decay widths for $B_{cc} \to B_c e^+ \nu_e$, where the dashed lines and band widths are the center values and uncertainties, while (a),(b),(c) and (d),(e),(f) correspond to the $c \to s$ and $c \to d$ transitions, respectively.

net result is that the tendencies of $P_{C,V}$ smear out each other in $\partial_q \Gamma$. In contrast, the behavior of $\partial_q \Gamma$ is dominated by P_V in $\Xi_{cc}^{++} \to \Xi_c'^+ e^+ \nu_e$. The sharp difference can be traced back to the spin-flavor overlappings, where we approximately have $P_C \propto N_{\text{unflip}}^2$ and $P_V \propto N_{\text{flip}}^2$. From Table I, we see that $(N_{\text{flip}}/N_{\text{unflip}})^2$ are 1/9 and 100/36 for $\Xi_{cc}^{++} \to \Xi_c^+$ and $\Xi_{cc}^{++} \to \Xi_c'^+$, respectively, which explains the opposite behaviors.

To test the lepton universality in the future experiments, we provide the ratios of

$$\mathcal{R} = \Gamma(B_{cc} \to B_c \mu^+ \nu_\mu)/\Gamma(B_{cc} \to B_c e^+ \nu_e)$$

in Table V. Their values are close to but below 1. Clearly, if $\mathcal{R} > 1$ in the future experiment, it will be a signal of new physics.
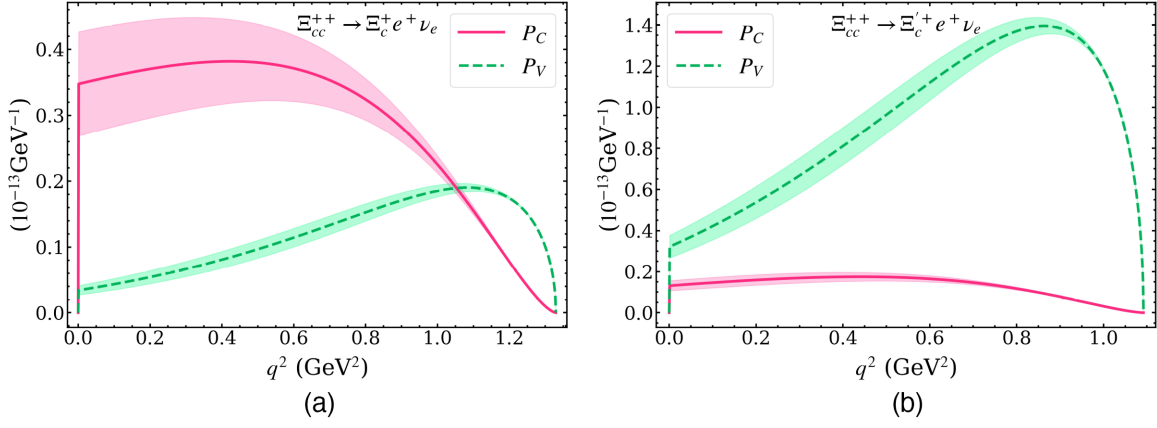
FIG. 5. The partial decay widths of P_C and P_C for $\Xi_{cc}^{++} \to \Xi_c^{(')+} e^+ \nu_e$.

To eliminate the uncertainties caused by V_{cf}, by defining

$$G_{B_c}^{B_{cc}} = \frac{1}{|V_{cf}|^2} \Gamma(B_{cc} \to B_c e^+ \nu_e), \qquad (18)$$

we find that

$$G_{\Xi_c^+}^{\Xi_{cc}^{++}} : G_{\Xi_c^0}^{\Xi_{cc}^+} : G_{\Lambda_c^+}^{\Xi_{cc}^{++}} : G_{\Xi_c^0}^{\Omega_{cc}^+} = 1 : 0.99 : 1.24 : 1.17,$$

$$G_{\Xi_c'^+}^{\Xi_{cc}^{++}} : G_{\Xi_c'^0}^{\Xi_{cc}^+} : \frac{1}{2} G_{\Omega_c^0}^{\Omega_{cc}^+} : G_{\Sigma_c^+}^{\Xi_{cc}^{++}} : G_{\Xi_c'^0}^{\Omega_{cc}^+} : \frac{1}{2} G_{\Sigma_c^+}^{\Xi_{cc}^+}$$

$$= 1 : 0.99 : 1.01 : 1.30 : 1.32 : 1.31, \qquad (19)$$

which are all expected to be 1 in the exact $SU(3)_F$ symmetry. As mentioned in the discussions of the form

factors early, the main $SU(3)_F$ breaking effects come from the phase space difference. For instance, from Fig. 4, the phase space of $\Xi_{cc}^{++} \to \Lambda_c^+$ is 1.3 times larger than the one of $\Xi_{cc}^{++} \to \Xi_c^+$, which partly explains the ratios in Eq. (19).

The computed decay widths, along with those in the literature, are shown in Table VI, where Ref. [22] computes the form factors by the MBM, Ref. [23] analyzes the decays with the heavy quark spin symmetry (HQSS), Refs. [26,41] adopt the LFQM with different sets of the parameter input, and Ref. [42] calculates the decay widths by the QCDSR. The decay width of $\Xi_{cc}^{++} \to \Xi_c^{(')+} e^+ \nu_e$ is slightly larger than the one of $\Xi_{cc}^+ \to \Xi_c^{(')0} e^+ \nu_e$ as $M_{\Xi_{cc}^{++}}$ is 2 MeV larger than $M_{\Xi_{cc}^+}$. For the $c \to s$ transition, our results of the decay widths are well consistent with the ones of the HQSS but systematically lower than those in the LFQM [41] and MBM [22] by a factor of 1.5. We note that in the MBM [22], the q^2 dependencies of the form factors are put in by hand and independent of the spectator quarks. For instance, the q^2 dependencies of $\Lambda_c \to \Lambda$ and $\Xi_{cc}^{++} \to \Xi_c^+$ are taken to be the same in the MBM [22]. However, we emphasize that the spectator effects of the charm quark and others are very different, as shown explicitly in D_q^v of Eq. (8). The exponential factor of $\exp(-2iE_c vz)$ deviates

TABLE V. The ratios $\mathcal{R}$.

$c \to s$	$\mathcal{R}$	$c \to d$	$\mathcal{R}$
$\Xi_{cc}^{++} \to \Xi_c^+$	0.99	$\Xi_{cc}^{++} \to \Lambda_c^+$	1.00
$\Xi_{cc}^+ \to \Xi_c^0$	0.99	$\Omega_{cc}^+ \to \Xi_c^0$	1.00
$\Xi_{cc}^{++} \to \Xi_c'^+$	0.97	$\Xi_{cc}^{++} \to \Sigma_c^+$	0.97
$\Xi_{cc}^+ \to \Xi_c'^0$	0.97	$\Omega_{cc}^+ \to \Xi_c'^0$	0.97
$\Omega_{cc}^+ \to \Omega_c^0$	0.97	$\Xi_{cc}^+ \to \Sigma_c^0$	0.97

TABLE VI. The decay widths in units of 10^{-14} GeV along with the ones in the literature.

$B_{cc} \to B_c e^+ \nu_e$	This work	MBM [22]	HQSS [23]	LFQM [26]	LFQM [41]	QCDSR [42]
$\Xi_{cc}^{++} \to \Xi_c^+ e^+ \nu_e$	5.11 ± 0.64	7.36	5.78	11.50	8.74	7.72 ± 3.70
$\Xi_{cc}^+ \to \Xi_c^0 e^+ \nu_e$	5.08 ± 0.64	7.36	5.73	11.40	8.63	7.72 ± 3.70
$\Xi_{cc}^{++} \to \Xi_c'^+ e^+ \nu_e$	10.92 ± 0.81	17.56	9.64	12.80	14.30	5.31 ± 3.52
$\Xi_{cc}^+ \to \Xi_c'^0 e^+ \nu_e$	10.85 ± 0.81	13.02	9.57	12.70	14.10	5.31 ± 3.52
$\Omega_{cc}^+ \to \Omega_c^0 e^+ \nu_e$	22.09 ± 1.63	26.76	18.61	25.50	28.00	12.50 ± 8.02
$\Xi_{cc}^{++} \to \Lambda_c^+ e^+ \nu_e$	0.34 ± 0.06	0.46	0.32	1.05	0.80	0.76 ± 0.37
$\Omega_{cc}^+ \to \Xi_c^0 e^+ \nu_e$	0.32 ± 0.04	0.46	0.27	0.81	0.59	0.61 ± 0.28
$\Xi_{cc}^{++} \to \Sigma_c^+ e^+ \nu_e$	0.76 ± 0.06	0.78	0.52	0.96	1.09	0.49 ± 0.29
$\Omega_{cc}^+ \to \Xi_c'^0 e^+ \nu_e$	0.77 ± 0.06	0.91	0.49	0.93	1.03	0.56 ± 0.35
$\Xi_{cc}^+ \to \Sigma_c^0 e^+ \nu_e$	1.52 ± 0.12	1.50	1.04	1.91	2.17	0.99 ± 0.58

largely to those of $\exp(-2iE_{u,d,s}vz)$. In particular, we find that it suppresses the decay widths by more than 40%, which causes the deviations between the results of the MBM and ours.

IV. CONCLUSION

We have studied the semileptonic decays of the doubly charmed baryons. Explicitly, we have found that $\Gamma(\Xi_{cc}^{++} \to \Xi_c^+ e^+ \nu_e, \Xi_c'^+ e^+ \nu_e, \Lambda_c^+ e^+ \nu_e, \Omega_c^+ e^+ \nu_e) = (5.1 \pm 0.1, 11 \pm 1, 0.34 \pm 0.06, 0.76 \pm 0.06) \times 10^{-14}$ GeV, $\Gamma(\Xi_{cc}^+ \to \Xi_c^0 e^+ \nu_e, \Xi_c'^0 e^+ \nu_e, \Sigma_c^0 e^+ \nu_e) = (5.1 \pm 0.6, 11 \pm 1, 1.5 \pm 0.1) \times 10^{-14}$ GeV, and $\Gamma(\Omega_{cc}^+ \to \Omega_c^0 e^+ \nu_e, \Xi_c^0 e^+ \nu_e, \Xi_c'^0 e^+ \nu_e) = (22 \pm 2, 0.32 \pm 0.04, 0.77 \pm 0.06) \times 10^{-14}$ GeV. We have discussed the $SU(3)_F$ breaking effects regarding the aspects of (i) the phase spaces differences, (ii) the spectator quark effects, and (iii) the overlappings of the transited quarks. We have shown that the other breaking effects are negligible compared to the phase space differences. In particular, the form factors well respect the $SU(3)_F$ relations

using ω as the variables. In addition, we have obtained that $\Gamma(\Xi_{cc}^{++} \to \Lambda_c^+ e^+ \nu_e)V_{cs}^2/\Gamma(\Xi_{cc}^{++} \to \Xi_c^+ e^+ \nu_e)V_{cd}^2 = 1.24$, which is expected to be 1 under the exact $SU(3)_F$ symmetry.

The behaviors of the parity violating and conserving partial decay widths have been examined. Accordingly, we have demonstrated that the partial decay width of $\Xi_{cc}^{++} \to \Xi_c^+ e^+ \nu_e$ is smoother than others, which can be testified in future experiments. We have also shown that the spectator effects of the charm quark suppress the decay widths by 40% and shall not be taken to be the same as the other quarks.

[1] M. Mattson *et al.* (SELEX Collaboration), Phys. Rev. Lett. **89,** 112001 (2002).

[2] A. Ocherashvili *et al.* (SELEX Collaboration), Phys. Lett. B **628,** 18 (2005).

[3] S. P. Ratti, Nucl. Phys. B, Proc. Suppl. **115,** 33 (2003).

[4] B. Aubert *et al.* (*BABAR* Collaboration), Phys. Rev. D **74,** 011103 (2006).

[5] Y. Kato *et al.* (Belle Collaboration), Phys. Rev. D **89,** 052003 (2014).

[6] R. Aaij *et al.* (LHCb Collaboration), Phys. Rev. Lett. **119,** 112001 (2017).

[7] R. Aaij *et al.* (LHCb Collaboration), Phys. Rev. Lett. **121,** 052002 (2018).

[8] R. Aaij *et al.* (LHCb Collaboration), Phys. Rev. Lett. **121,** 162002 (2018).

[9] Q. F. Lü, K. L. Wang, L. Y. Xiao, and X. H. Zhong, Phys. Rev. D **96,** 114006 (2017).

[10] L. Y. Xiao, K. L. Wang, Q. f. Lu, X. H. Zhong, and S. L. Zhu, Phys. Rev. D **96,** 094005 (2017).

[11] L. Meng, H. S. Li, Z. W. Liu, and S. L. Zhu, Eur. Phys. J. C **77,** 869 (2017).

[12] M. Z. Liu, Y. Xiao, and L. S. Geng, Phys. Rev. D **98,** 014040 (2018).

[13] A. Ali, Q. Qin, and W. Wang, Phys. Lett. B **785,** 605 (2018).

[14] A. V. Berezhnoy, A. K. Likhoded, and A. V. Luchinsky, Phys. Rev. D **98,** 113004 (2018).

[15] D. L. Yao, Phys. Rev. D **97,** 034012 (2018).

[16] J. M. Dias, V. R. Debastiani, J. J. Xie, and E. Oset, Phys. Rev. D **98,** 094017 (2018).

[17] L. Y. Xiao, Q. F. Lü, and S. L. Zhu, Phys. Rev. D **97,** 074005 (2018).

[18] X. H. Hu, Y. L. Shen, W. Wang, and Z. X. Zhao, Chin. Phys. C **42,** 123102 (2018).

[19] Y. L. Ma and M. Harada, J. Phys. G **45,** 075006 (2018).

[20] L. Meng and S. L. Zhu, Phys. Rev. D **100,** 014006 (2019).

[21] U. Özdem, J. Phys. G **46,** 035003 (2019).

[22] R. Perez-Marcial, R. Huerta, A. Garcia, and M. Avila-Aoki, Phys. Rev. D **40,** 2955 (1989).

[23] C. Albertus, E. Hernández, and J. Nieves, Phys. Lett. B **704,** 499 (2011).

[24] N. Sharma and R. Dhir, Phys. Rev. D **96,** 113006 (2017).

[25] T. Gutsche, M. A. Ivanov, J. G. Körner, and V. E. Lyubovitskij, Phys. Rev. D **96,** 054013 (2017).

[26] W. Wang, F. S. Yu, and Z. X. Zhao, Eur. Phys. J. C **77,** 781 (2017).

[27] W. Wang, Z. P. Xing, and J. Xu, Eur. Phys. J. C **77,** 800 (2017).

[28] F. S. Yu, H. Y. Jiang, R. H. Li, C. D. Lü, W. Wang, and Z. X. Zhao, Chin. Phys. C **42,** 051001 (2018).

[29] H. S. Li, L. Meng, Z. W. Liu, and S. L. Zhu, Phys. Lett. B **777,** 169 (2018).

[30] L. J. Jiang, B. He, and R. H. Li, Eur. Phys. J. C **78,** 961 (2018).

[31] Q. A. Zhang, Eur. Phys. J. C **78,** 1024 (2018).

[32] R. Dhir and N. Sharma, Eur. Phys. J. C **78,** 743 (2018).

[33] R. H. Li and C. D. Lu, arXiv:1805.09064.

[34] Y. J. Shi, W. Wang, Y. Xing, and J. Xu, Eur. Phys. J. C **78,** 56 (2018).

[35] Y. Xing and R. Zhu, Phys. Rev. D **98,** 053005 (2018).

[36] Z. P. Xing and Z. X. Zhao, Phys. Rev. D **98,** 056002 (2018).

[37] Z. X. Zhao, Eur. Phys. J. C **78,** 756 (2018).

[38] T. Gutsche, M. A. Ivanov, J. G. Körner, V. E. Lyubovitskij, and Z. Tyulemissov, Phys. Rev. D **99,** 056013 (2019).

[39] Y. J. Shi, Y. Xing, and Z. X. Zhao, Eur. Phys. J. C **79**, 501 (2019).

[40] X. H. Hu and Y. J. Shi, Eur. Phys. J. C **80**, 56 (2020).

[41] X. H. Hu, R. H. Li, and Z. P. Xing, Eur. Phys. J. C **80**, 320 (2020).

[42] Y. J. Shi, W. Wang, and Z. X. Zhao, Eur. Phys. J. C **80**, 568 (2020).

[43] R. Zhu, X. L. Han, Y. Ma, and Z. J. Xiao, Eur. Phys. J. C **78**, 740 (2018).

[44] C. Q. Geng, C. W. Liu, and T. H. Tsai, Phys. Rev. D **102**, 034033 (2020).

[45] C. W. Liu and C. Q. Geng, J. High Energy Phys. 01 (2022) 128.

[46] C. Q. Geng, X. N. Jin, and C. W. Liu, Phys. Rev. D **106**, 053006 (2022).

[47] C. Q. Geng, X. N. Jin, and C. W. Liu, Phys. Rev. D **107**, 033008 (2023).

[48] J. Zhang, X. N. Jin, C. W. Liu, and C. Q. Geng, Phys. Rev. D **107**, 033004 (2023).

[49] C. W. Liu and C. Q. Geng, Chin. Phys. C **47**, 014104 (2023).

[50] A. Kadeer, J. G. Korner, and U. Moosbrugger, Eur. Phys. J. C **59**, 27 (2009).

[51] C. Q. Geng, C. W. Liu, T. H. Tsai, and S. W. Yeh, Phys. Lett. B **792**, 214 (2019).

[52] J. G. Korner, M. Kramer, and D. Pirjol, Prog. Part. Nucl. Phys. **33**, 787 (1994).

[53] R. L. Workman *et al.* (Particle Data Group), Prog. Theor. Exp. Phys. **2022**, 083C01 (2022).

[54] W. X. Zhang, H. Xu, and D. Jia, Phys. Rev. D **104**, 114011 (2021).